High performance separator coated with amino-functionalized SiO$_2$ particles for safety enhanced lithium-ion batteries

Jinhyun Cho[a], Yun-Chae Jung[a], Yun Sung Lee[b], Dong-Won Kim[a],*

[a] *Department of Chemical Engineering, Hanyang University, Seungdong-Gu, Seoul 04763, Republic of Korea*
[b] *Faculty of Chemical Engineering, Chonnam National University, Buk-Gu Gwangju 61186, Republic of Korea*

ARTICLE INFO

ABSTRACT

Amino-functionalized SiO$_2$ (N-SiO$_2$) particles were synthesized and used to coat both sides of a porous polyethylene separator. The N-SiO$_2$ coated separator exhibited good wettability by liquid electrolyte, high ionic conductivity when soaked with liquid electrolyte and enhanced thermal stability at high temperatures. By employing the N-SiO$_2$ coated separator in fabricating the lithium-ion cell composed of a graphite negative electrode and a LiNi$_{1/3}$Co$_{1/3}$Mn$_{1/3}$O$_2$ positive electrode, its cycling stability was improved compared to a cell assembled with either a conventional polyethylene separator or a SiO$_2$ coated polyethylene separator. The N-SiO$_2$ coated separator is a promising separator to enhance the cycling stability and thermal safety of lithium-ion battery.

1. Introduction

Lithium-ion batteries have successfully enabled the widespread use of portable electronic devices, power tools and electric vehicles [1–4]. In these batteries, a separator is a crucial component that functions as a physical barrier between two electrodes as well as an electrolyte reservoir for ionic transport within the cell. Most of the separators currently used in commercialized lithium-ion batteries are based on polyolefins such as polyethylene (PE) and polypropylene (PP) [5–7]. Although these separators offer excellent mechanical strength and chemical stability, they shrink and even melt at high temperature, which causes a short circuit between two electrodes in the case of unusual heat generation [8,9]. Furthermore, their hydrophobic nature leads to incomplete filling of pores in the separator with liquid electrolyte, which results in high ionic resistance [10–12]. Therefore, a high performance separator with good wettability and enhanced thermal stability is imperative and highly desirable, particularly in the large-scale lithium-ion batteries designed for electric vehicles and energy storage systems. In this regard, ceramic-coated separators or inorganic-based separators have been developed by combining characteristics of polymeric separator and ceramic materials [13–24]. In the ceramic-coated separators, commercially available inorganic particles such as SiO$_2$ and Al$_2$O$_3$ are coated with polymer binder on the surface of the polyolefin separator [13–20]. The coating of ceramic particles has been effective in improving the mechanical, thermal and electrical properties of polyolefin separators. The inorganic-based separators

exhibited excellent thermal stability, high electrolyte absorption and no dendrite puncturing problems as compared with polyolefin separators, which makes it possible to fabricate a safety enhanced battery [21–24].

In this study, we synthesized amino-functionalized SiO$_2$ particles (N-SiO$_2$) that are more compatible with carbonate-based liquid electrolytes. The N-SiO$_2$ particles were then coated with polymer binder onto both sides of a porous PE separator. Due to the high affinity of N-SiO$_2$ with liquid electrolyte, the N-SiO$_2$ coated separator exhibited good wettability by liquid electrolyte and high ionic conductivity when soaked with liquid electrolyte. Additionally, the N-SiO$_2$ particles on the PE separator played a role as a HF scavenger, which suppressed the electrolyte decomposition at elevated temperature. The N-SiO$_2$ coated separator was used to fabricate the cell composed of a graphite negative electrode and a LiNi$_{1/3}$Co$_{1/3}$Mn$_{1/3}$O$_2$ positive electrode. Cycling performance of the lithium-ion cell with the N-SiO$_2$ coated separator was evaluated and compared to those of cells employing conventional PE separator or SiO$_2$ coated PE separator.

2. Experimental

2.1. Synthesis of amino-functionalized SiO$_2$ particles

SiO$_2$ particles were synthesized by the hydrolysis and condensation of tetraethyl orthosilicate (TEOS, Sigma-Aldrich) in an aqueous solution, as schematically illustrated in Fig. 1. An appropriate amount of
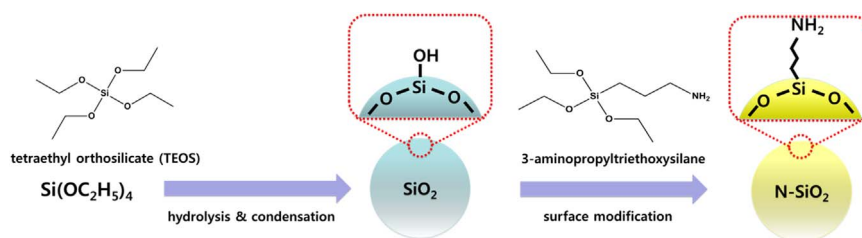
Fig. 1. Schematic illustration of the synthesis of SiO$_2$ and amino-functionalized SiO$_2$ (N-SiO$_2$) particles.

TEOS was added to a distilled water and ethanol mixture while stirring until the TEOS droplets completely disappeared in the solution. A catalytic amount of NH$_4$OH in water (28 wt%, Junsei) was added to the solution, and the hydrolysis and condensation reaction was allowed to proceed for 2 h at ambient temperature. After 2 h, the resulting precipitate was centrifuged and washed several times with distilled water and ethanol. SiO$_2$ particles were obtained after vacuum drying at 110 °C for 12 h.

To functionalize the SiO$_2$ particles with amino groups, the SiO$_2$ particles were dispersed in methanol via ultrasonication for 30 min, and 3-aminopropyltriethoxysilane (Sigma-Aldrich) was added to the solution. After reaction for 2 h at room temperature, the product was centrifuged and washed several times with methanol. The N-SiO$_2$ particle was obtained as a white powder after vacuum drying at 110 °C for 12 h.

2.2. Preparation of the N-SiO$_2$ coated separator

The N-SiO$_2$ coated separator was prepared from N-SiO$_2$ particles and poly(vinylidene fluoride-co-hexafluoropropylene) (P(VdF-co-HFP), Kynar 2801) copolymer. P(VdF-co-HFP) was dissolved in dimethylformamide (DMF), and the N-SiO$_2$ particles were directly added to the polymer solution. The weight ratio of N-SiO$_2$ particles to P(VdF-co-HFP) was 30: 70. The coating slurry was uniformly mixed by ball milling for 24 h. The resulting slurry was coated onto both sides of a PE separator (Asahi-Kasei Co., thickness: 20 μm). The separator was dried at room temperature for 30 min to allow the solvent to evaporate, followed by additional drying in a vacuum oven at 80 °C for 24 h. For comparison, the SiO$_2$ coated separator was similarly prepared by coating SiO$_2$ particles and P(VdF-co-HFP) (30:70 by weight) onto both sides of the PE separator. The total thickness of the ceramic-coated separators (SiO$_2$ coated and N-SiO$_2$ coated separators) was maintained at about 25 μm.

2.3. Cell assembly

As a cathode active material, LiNi$_x$Co$_y$Mn$_z$O$_2$ (NCM) has higher specific capacity than LiCoO$_2$ and similar operating voltage while having lower cost. LiNi$_{1/3}$Co$_{1/3}$Mn$_{1/3}$O$_2$ is the common form of NCM and is being widely used in commercialized lithium-ion batteries. Thus, LiNi$_{1/3}$Co$_{1/3}$Mn$_{1/3}$O$_2$ was chosen as an active material in positive electrode. The positive electrode was prepared by doctor-blade casting of a slurry composed of 85 wt% LiNi$_{1/3}$Co$_{1/3}$Mn$_{1/3}$O$_2$ (3 M Co.), 7.5 wt% poly(vinylidene fluoride) (PVdF) and 7.5 wt% super-P carbon (MMM Co.) onto aluminum foil. The mass of LiNi$_{1/3}$Co$_{1/3}$Mn$_{1/3}$O$_2$ in the positive electrode corresponded to a capacity of about 2.0 mAh cm^{-2}. The negative electrode was similarly prepared by coating copper foil with the NMP-based slurry of mesocarbon microbeads (MCMB), PVdF and super-P carbon (88:8:4 by weight). A liquid electrolyte consisting of 1.15 M LiPF$_6$ in ethylene carbonate (EC)/ethylmethyl carbonate (EMC) (3:7 by volume, battery grade) containing 5.0 wt% fluoroethylene carbonate (FEC) was kindly supplied by PANAX ETEC Co. Ltd. and was used as received. FEC was added into the electrolyte solution in order to form stable solid electrolyte interphase (SEI) layer on the electrode surface, which resulted in improvement of cycling stability [25]. Karl Fisher titration using Mettler-Toledo Coulometer confirmed

that the water content in the liquid electrolyte was less than 20 ppm. A lithium-ion cell was assembled by sandwiching the N-SiO$_2$ coated separator between the graphite negative electrode and the LiNi$_{1/3}$Co$_{1/3}$Mn$_{1/3}$O$_2$ positive electrode. The cell was enclosed in a pouch injected with liquid electrolyte and was then vacuum-sealed. Approximately, 1.46 g of electrolyte solution was injected into a pouch cell with a dimension of 3×5 cm^2. For comparison, the lithium-ion cells with conventional PE separator and SiO$_2$ coated PE separator were also assembled employing the same liquid electrolyte. All cells were assembled in an argon-filled glove box in which the moisture and oxygen content were less than 1 ppm.

2.4. Characterization and measurements

The morphologies of silica particles (SiO$_2$, N-SiO$_2$) and various separators were examined using a field emission scanning electron microscope (FE-SEM, JEOL JSM-6330F). The functional group on the surface of the N-SiO$_2$ particles was examined using X-ray photoelectron spectroscopy (XPS). XPS measurements were conducted on a Thermo VG Scientific ESCA 2000 system using an Al Kα radiation source. Elemental analyzer (FLASH® EA1112) was used to measure the amount of nitrogen in amino-functionalized silica. The mechanical properties of various separators were measured using a universal test machine (Instron 5966) in accordance with the ASTM D882 method. In order to measure the electrolyte uptake and ionic conductivity, the separators were immersed in the liquid electrolyte for 1 h. Afterward, the separators were taken out of the electrolyte solution, and excess electrolyte solution on the surface of the separator was removed by wiping with filter paper. The uptake of the electrolyte solution was then determined using Eq. (1),

$$\text{Electrolyte uptake (\%)} = (W - W_o)/W_o \times 100 \qquad (1)$$

where W_o and W are the weights of the separator before and after soaking in the liquid electrolyte, respectively [26,27]. The separator soaked with liquid electrolyte was sandwiched between two stainless steel electrodes for conductivity measurements. AC impedance measurements were carried out in the frequency range of 1 mHz to 100 kHz with an amplitude of 10 mV using a Zahner Electrik IM6 impedance analyzer. The thermal shrinkage of the separators was measured in terms of their dimensional changes after being held for 30 min at 130 °C. Charge and discharge cycling tests of the lithium-ion cells were conducted at current density of 1.0 mA cm^{-2} (0.5 C rate) over the voltage range from 3.0 to 4.5 V using battery test equipment (WBCS 3000, Wonatech) at 25 and 55 °C, respectively. Various C rates were also applied to evaluate the rate capabilities of the cells. Surface characterization of the graphite negative electrodes after 100 cycles at 55 °C was conducted using XPS. The electrode was washed several times with anhydrous dimethyl carbonate to remove residual electrolyte, followed by vacuum drying overnight at room temperature. The HF content in the electrolyte was measured using an acid–base titration method after the fresh cell was stored in a 55 °C oven for three days [28]. Methyl orange was used as an acid–base indicator.
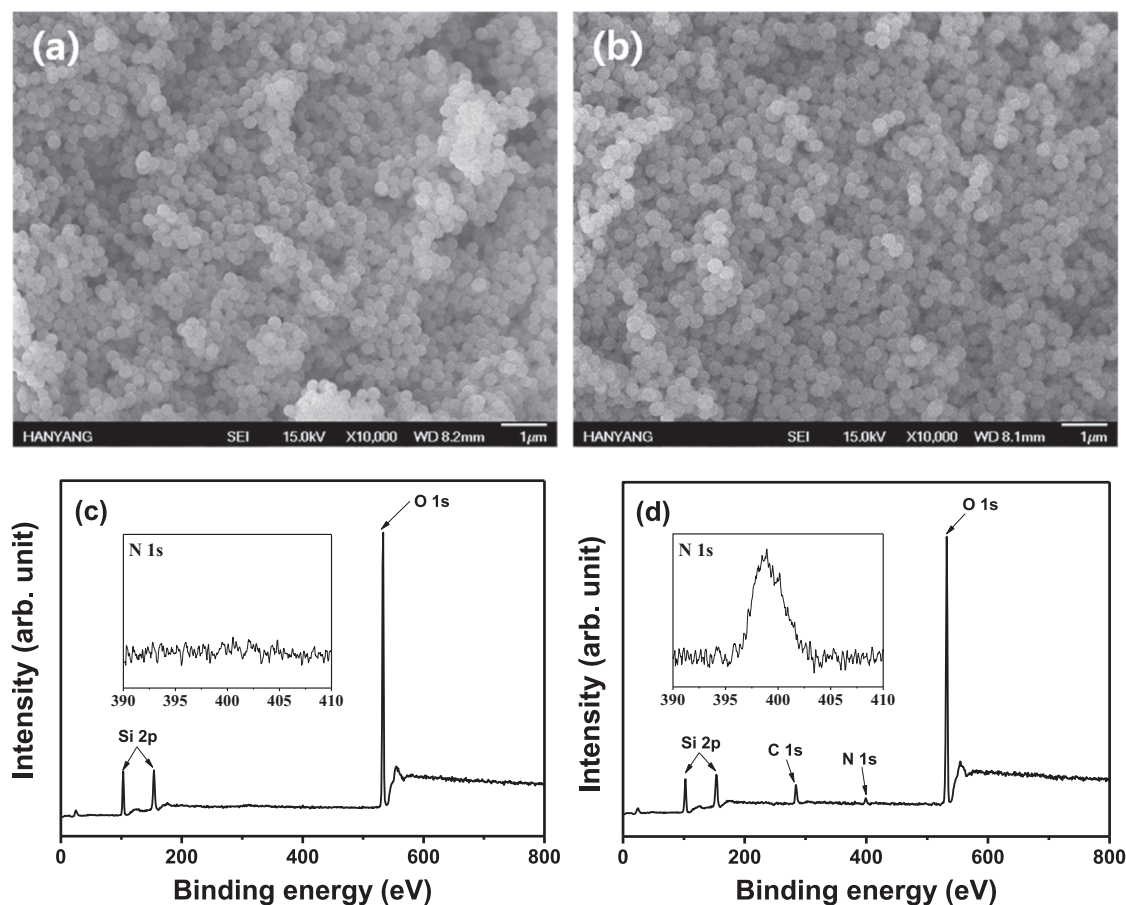
Fig. 2. FE-SEM images of (a) SiO$_2$ particles and (b) N-SiO$_2$ particles. XPS spectra of (c) SiO$_2$ particles and (d) N-SiO$_2$ particles.

3. Results and discussion

Fig. 2(a) and (b) show the FE-SEM images of SiO$_2$ and N-SiO$_2$ particles. All silica particles had uniform spherical shapes with an average diameter of 300 nm. The incorporation of amino groups on the SiO$_2$ particles did not affect their particle size. In the XPS spectra of SiO$_2$ and N-SiO$_2$ particles (Fig. 2(c) and (d)), an additional small peak was observed near 399.1 eV for the N-SiO$_2$ particles only, which corresponds to the N 1 s peak [29], indicating that the SiO$_2$ particles were successfully functionalized with amino groups. From the elemental analysis, the amount of amino groups in the N-SiO$_2$ particles was measured to be about 0.48 wt%.

The synthesized silica particles (SiO$_2$ and N-SiO$_2$) were used to coat both sides of PE separator to obtain ceramic-coated separators. The FE-SEM images of the pristine PE separator and ceramic-coated separators are presented in Fig. 3. The pristine PE separator showed a uniformly interconnected and submicron pore structure (Fig. 3(a)). When silica particles (SiO$_2$ and N-SiO$_2$) were coated onto the PE separator, they were uniformly distributed on the surface, irrespective of the type of silica particles (Fig. 3(b) and (c)). As shown in Fig. 3(d), the coating layer firmly adhered to the surface of the PE separator, and its thickness was measured to be about 2.5 μm on each side. The density of N-SiO$_2$ coated separator (0.57 g cm^{-3}) was slightly lower than that of pristine PE separator (0.59 g cm^{-3}), which was due to the presence of porous coating layer in the N-SiO$_2$ coated separator.

The electrolyte uptake and ionic conductivities of various separators soaked with liquid electrolyte are summarized in Table 1. As expected, the PE separator exhibited lower electrolyte uptake due to its inherent hydrophobic nature. For the ceramic-coated separators, the amount of electrolyte absorbed was greater than that absorbed by the PE separator, which resulted in higher ionic conductivity. For the pristine PE separator, the electrolyte solution can only be trapped in inner pores, which results in low electrolyte uptake. In the case of the ceramic-coated separators, liquid electrolyte can be trapped not only in the inner pores of the supporting PE separator, but can also be retained in the coating layer formed by the hydrophilic SiO$_2$ particles and the P(VdF-co-HFP) copolymer.

Note that both electrolyte uptake and ionic conductivity were higher in the N-SiO$_2$ coated separator than in the SiO$_2$ coated separator. This result was due to the presence of amino groups on the surface of SiO$_2$ particles in the N-SiO$_2$ coated separator, because the amino groups were highly compatible with the polar electrolyte solution. These results demonstrate that the surface modification of the PE separator with the N-SiO$_2$ particles is effective in enhancing electrolyte uptake and ionic conductivity compared to the conventional PE or SiO$_2$-coated separators.

Contact angle with water droplet was measured to compare the wettability of the separators, and the results are shown in Fig. 4(a). It is evident that the surface coating of the PE separator with SiO$_2$ particles decreased the contact angle from 96.3° to 68.5°, indicating that the SiO$_2$ coated separator became more hydrophilic due to the presence of SiO$_2$ particles and P(VdF-co-HFP) on the surface of the PE separator. The surface coating of the PE separator with N-SiO$_2$ particles further decreased the contact angle to 51.3°. This result is due to the fact that the amino group is hydrophilic and has good affinity for polar solvent. Because the manufacturing process of the PE separator includes biaxial stretching, they readily lose dimensional stability upon exposure to high temperatures near their melting temperature. Thus, it is important to maintain their dimension at high temperatures in order to prevent an electric short circuit between two electrodes within the cell, the failure of which may eventually lead to fire or explosion under unusual conditions such as abnormal heating and mechanical rupture. To
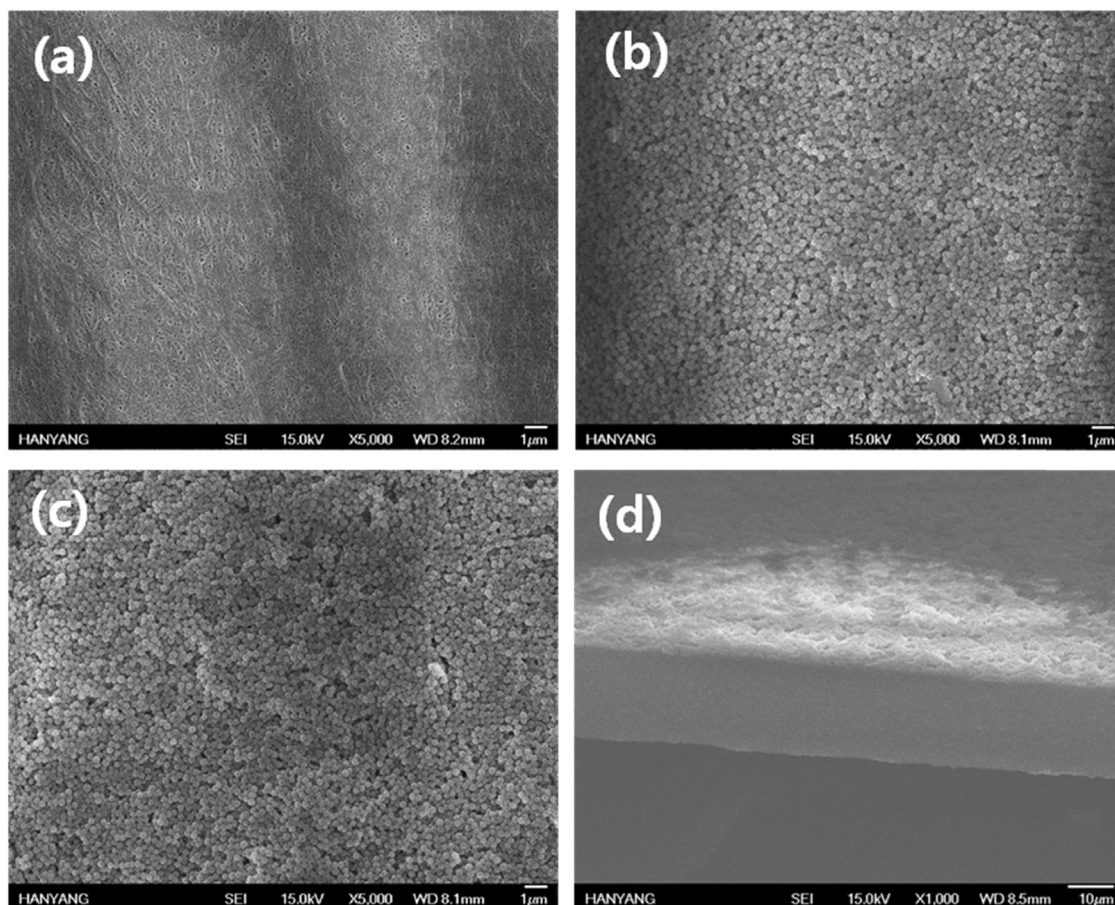
Fig. 3. FE-SEM images of (a) PE, (b) SiO₂ coated and (c) N-SiO₂ coated separators. (d) Cross-sectional SEM image of N-SiO₂ coated separator.

Table 1
Electrolyte uptake and ionic conductivities of various separators when soaked with liquid electrolyte.

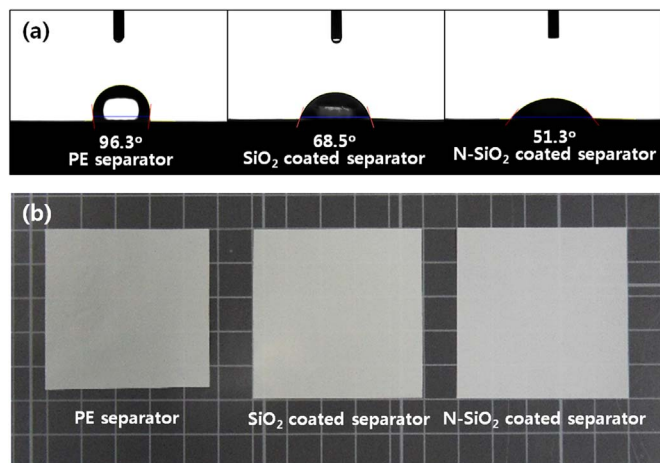| Separator	Thickness (μm)	Electrolyte uptake (%)	Ionic conductivity (S cm^{-1})
PE separator	20	98.3	4.2×10^{-4}
SiO₂ coated separator	25	178.1	6.9×10^{-4}
N-SiO₂ coated separator	25	195.4	8.1×10^{-4}

Fig. 4. (a) Contact angle images of different types of separators, and (b) photographs of different separators after exposure for 30 min at 130 °C.

evaluate the thermal stability of pristine PE and ceramic-coated separators, their thermal shrinkage behavior was examined after storing them for 30 min at 130 °C. As shown in Fig. 4(b), the pristine PE separator experienced a high degree of shrinkage (13.5%) after high-temperature exposure. In contrast, the separators coated with SiO₂ and N-SiO₂ inorganic particles did not exhibit thermal shrinkage regardless of the type of silica particle when exposed to the same conditions. This result is attributed to the incorporation of thermally-resistant SiO₂ or N-SiO₂ particles on both sides of the PE separator, helping to prevent thermal shrinkage of the separator at high temperature. When further increasing temperature, the N-SiO₂ coated separator showed a thermal shrinkage of about 10% at 150 °C.

With respect to mechanical properties, the tensile strength of N-SiO₂ coated separator (156.8 MPa) was almost same to that (160.1 MPa) of pristine PE separator. This result suggests that the surface coating of N-SiO₂ particles onto PE separator hardly affects its mechanical strength.

Cycling performance of lithium-ion cells assembled with different separators was evaluated. The cells were initially subjected to pre-conditioning cycles in the voltage range of 3.0–4.5 V at constant current rate of 0.1 C. After two cycles at 0.1 C, the cells were charged at current density of 0.5 C up to a cut-off voltage of 4.5 V. This was followed by a constant-voltage charge with decreasing current until a final current equal to 10% of the charging current was obtained. The cells were then discharged to a cut-off voltage of 3.0 V at the same current density. Fig. 5(a) shows the charge and discharge curves of the lithium-ion cell assembled with N-SiO₂ coated separator. The cell had an initial discharge capacity of 176.3 mAh g^{-1} based on the active LiNi$_{1/3}$Co$_{1/3}$Mn$_{1/3}$O₂ material in the positive electrode. After 200 cycles, the cell delivered a discharge capacity of 156.0 mAh g^{-1}. Fig. 5(b) shows the discharge capacities of lithium-ion cells with different separators as a function of cycle number. The initial discharge capacities of the cells
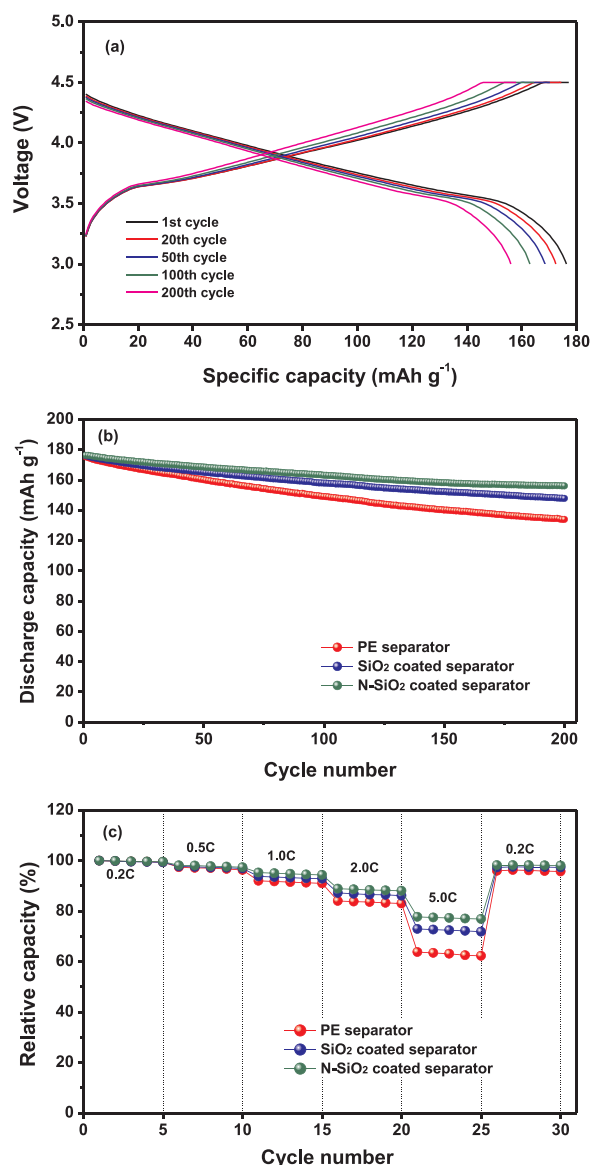
Fig. 6. AC impedance spectra of lithium-ion cells assembled with different separators measured (a) before and (b) after 200 cycles.

Fig. 5. (a) Charge and discharge curves of a lithium-ion cell assembled with a N-SiO$_2$ coated separator (0.5 C CC and CV charge, 0.5 C CC discharge, cut-off: 3.0–4.5 V, 25 °C). (b) Discharge capacities of lithium-ion cells with different separators as a function of cycle number. (c) Relative discharge capacities of lithium-ion cells with different separators as a function of C rate at 25 °C.

were nearly the same, irrespective of the type of the separator. From the initial discharge capacities, their energy densities were calculated without considering pouch weight. As a result, the energy density of the cell assembled with N-SiO$_2$ coated separator (259 Wh kg^{-1}) was relatively lower than that of cell with pristine PE separator (265 Wh kg^{-1}), which can be ascribed to the presence of additional coating layer in the N-SiO$_2$ coated separator. However, the cycling stability of the cell with N-SiO$_2$ coated separator was greatly enhanced, as depicted in Fig. 5(b). The improved cycling stability in the cell employing ceramic-coated separator may be caused by the enhanced retention ability of liquid electrolyte due to coating the PE separator with P(VdF-*co*-HFP) and SiO$_2$ or N-SiO$_2$ particles, which helped prevent exudation of the electrolyte solution during repeated cycling. Furthermore, the presence of SiO$_2$ or N-SiO$_2$ particles in the ceramic-coated separator can stabilize the electrolyte solution by absorbing some impurities, such as H$_2$O and HF [30,31], thereby suppressing the side reactions during cycling. As a result, the cells with ceramic-coated separators exhibited more stable cycling behavior. The rate capability
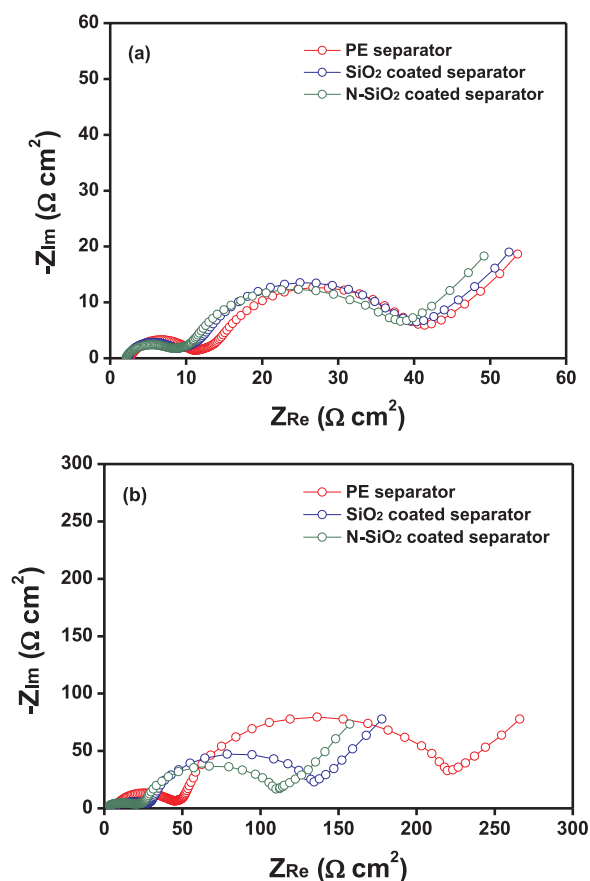
of the cells with different separators was evaluated at various current rates. The discharge capacities of the cells were measured during experiments in which the C rate increased gradually every five cycles within the range of 0.2–5.0 C, as shown in Fig. 5(c). In this figure, the relative capacity is defined as the ratio of the discharge capacity at a specific C rate to the initial discharge capacity delivered at a 0.2 C rate.

The discharge capacities of the lithium-ion cell assembled with N-SiO$_2$ coated separator were the greatest for all C rates tested. As discussed above, the ionic conductivity is the highest in the N-SiO$_2$ coated separator soaked with liquid electrolyte, thereby reducing the concentration polarization of the electrolyte during cycling. The gelation of P(VdF-*co*-HFP) with liquid electrolyte is also expected to assist in retaining the firm adhesion of the separator to the electrodes in the cell, facilitating the migration of lithium ions at the electrode-electrolyte interface during repeated cycling.

The electrochemical characteristics of the lithium-ion cells with different separators were investigated by AC impedance analysis before and after cycling, and the results are shown in Fig. 6. All spectra exhibited two overlapping semicircles, which can be ascribed to the resistance of Li$^+$ ions through the solid electrolyte interphase (SEI) at the electrode surface, and to the charge transfer resistance at the electrode-electrolyte interface [32–34]. Before cycling at a 0.5 C rate, the cells with different separators had nearly identical AC impedance spectra, indicating that the presence of the coating layer had little effect on the initial impedance of the cell. After the repeated cycling, the interfacial resistances increased for all of the cells. It is noticeable that the cell with the N-SiO$_2$ coated separator exhibited the smallest increase of interfacial resistances. This result can be ascribed to effective encapsulation of the electrolyte solution within the cell employing the N-SiO$_2$ coated separator, which also allowed facile charge transfer reaction at the electrode-electrolyte interface. Additionally, trace
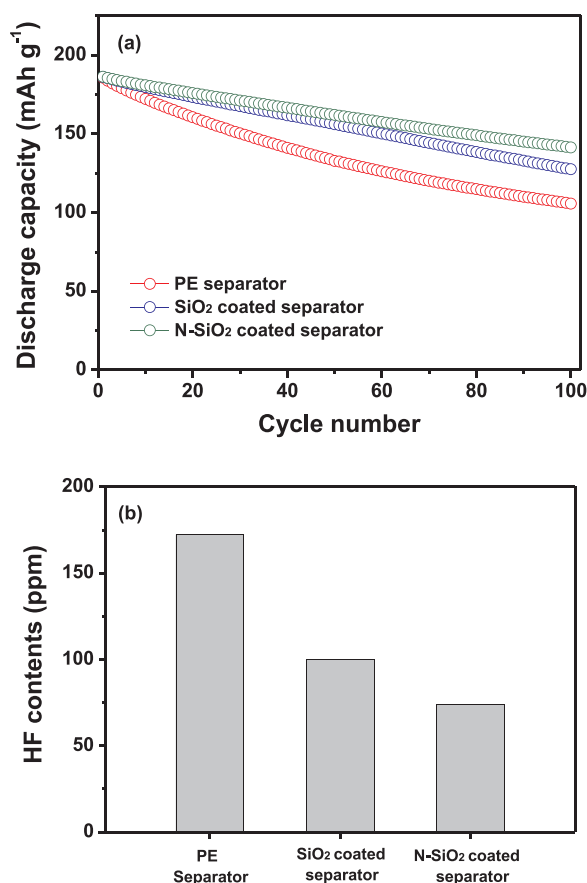
Fig. 7. (a) Discharge capacities of lithium-ion cells with different separators at 55 °C (0.5 C CC and CV charge, 0.5 C CC discharge, cut-off: 3.0–4.5 V). (b) HF content in the cells assembled with different separators after storage at 55 °C for 3 days.

amounts of acidic impurities and moisture in the electrolyte could be captured by N-SiO$_2$ particles, which suppressed deleterious reactions between the electrolyte solution and electrodes, resulting in improved interfacial stability. This result is consistent with previous works showing that the addition of inorganic filler was effective in stabilizing the electrode interfacial resistance [35,36].

A cycling test was also performed at 55 °C to compare the cycling stability of the cells at high temperature. Fig. 7(a) shows the discharge capacities of the lithium-ion cells with different separators as a function of the cycle number at 55 °C. It can be seen that the cell with the PE separator suffered from large capacity fading. In contrast, the cells assembled with ceramic-coated separators exhibited better capacity retention. Among the cells investigated, the cell assembled with N-SiO$_2$ coated separator exhibited the best capacity retention. It is well known that layered cathode materials experience gradual capacity fading at high temperatures due to structural and interfacial instabilities as well as dissolution of transition metals from the cathode material by HF attack [37,38]. Accordingly, the differences in high-temperature cycling stability of the cells can be closely related to the content of HF in the electrolyte. HF is generated by thermal decomposition and hydrolysis of LiPF$_6$ by trace moisture in the electrolyte solution [39,40]. HF content in the cells with different separators was measured after storing the fresh cell without cycling at 55 °C for 3 days. As depicted in Fig. 7(b), the HF content was significantly reduced in the cell with the N-SiO$_2$ coated separator. It is well known that SiO$_2$ particles can serve as HF scavengers to remove HF in the electrolyte solution as a result of formation of strong Si–F bonds by nucleophilic substitution reaction of HF [41]. Additionally, the amino group in the N-SiO$_2$ particles is a Lewis base and thus can effectively complex with thermally decomposed PF$_5$, which is a Lewis acid [42], thereby preventing hydrolysis to
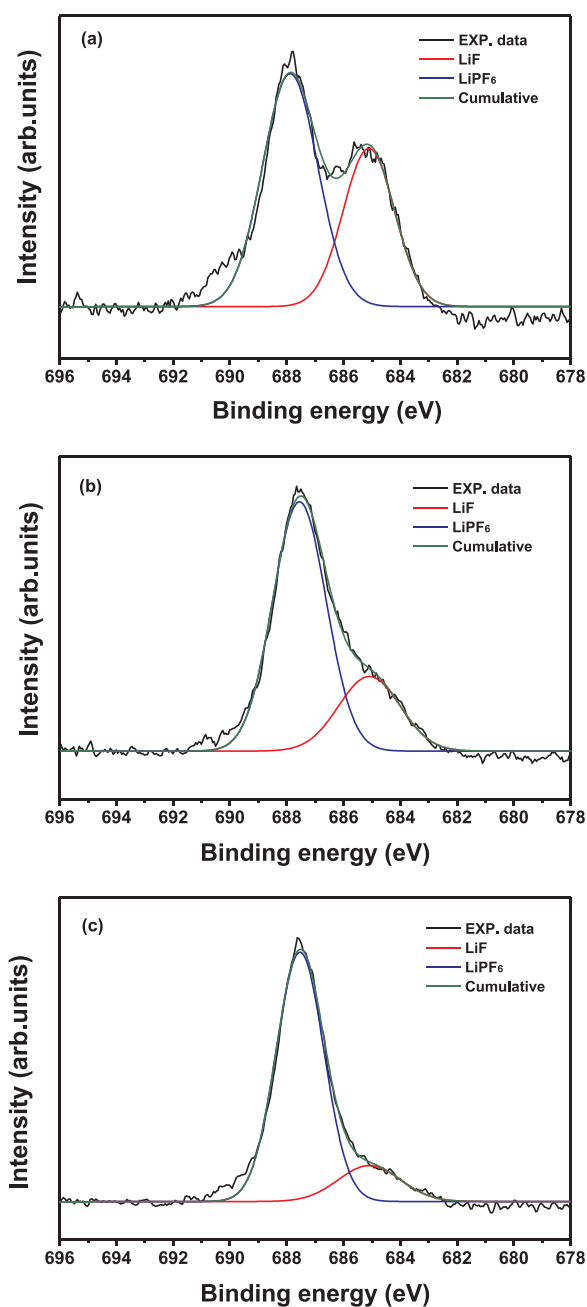

Fig. 8. F 1 s XPS spectra of graphite electrodes in the lithium-ion cells assembled with (a) PE, (b) SiO$_2$ coated, and (c) N-SiO$_2$ coated separators after 100 cycles at 55 °C.

produce HF.

Li et al. reported that the addition of Lewis basic additives could stabilize organic electrolytes against thermal decomposition initiated by Lewis acids [43]. Consequently, the use of the N-SiO$_2$ coated separator reduced the HF content and thus suppressed the dissolution of transition metals from the active LiNi$_{1/3}$Co$_{1/3}$Mn$_{1/3}$O$_2$ material at elevated temperatures. As a result, the cell assembled with the N-SiO$_2$ coated separator exhibited the most stable cycling behavior at 55 °C. In the case of the cell with a pristine PE separator, the dissolution of transition metals by HF attack may cause a rapid increase in the interfacial resistance, thereby accelerating the capacity loss as cycling progresses at elevated temperatures.

The surface of the graphite negative electrodes in cells with different separators was analyzed by F 1 s XPS after 100 cycles at 55 °C, and the results are shown in Fig. 8. The relative peak intensity of LiF observed at 685.1 eV was the smallest on the electrode surface of

the cell with the N-SiO$_2$ coated separator. LiF can be produced by thermal decomposition of LiPF$_6$ salt on the electrode surface [39]. It is an insulating material for both electrons and Li$^+$ ions; thus, the LiF that forms on the surface of the electrode may hamper the charge transfer reaction between the electrode and electrolyte, thereby increasing the charge transfer resistance. This result suggests that the N-SiO$_2$ coated separator was effective in suppressing the electrolyte decomposition at high temperature, which gives superior capacity retention at high temperature.

4. Conclusions

To develop a high performance separator with enhanced thermal stability and good cycling performance, amino-functionalized SiO$_2$ particles were synthesized and coated on both sides of a PE separator. Compared to a commercial PE separator, the N-SiO$_2$ coated separator exhibited good wettability by liquid electrolyte, high ionic conductivity when soaked with liquid electrolyte and excellent thermal stability at high temperature. A lithium-ion cell employing the N-SiO$_2$ coated separator showed superior cycling performance in terms of capacity retention, rate capability and high-temperature cycling stability compared to a cell prepared with a conventional PE separator or a SiO$_2$ coated separator. Our results demonstrate that the N-SiO$_2$ coated separator studied in this work can be a promising separator in rechargeable lithium-ion cells that require good cycling stability and enhanced thermal safety.

Acknowledgements

References

[1] J.B. Goodenough, Y. Kim, Challenges for rechargeable Li batteries, Chem. Mater. 22 (2010) 587–603.

[2] V. Etacheri, R. Marom, R. Elazari, G. Salitra, D. Aurbach, Challenges in the development of advanced Li-ion batteries: a review, Energy Environ. Sci. 4 (2011) 3243–3262.

[3] D. Larcher, J.-M. Tarascon, Towards greener and more sustainable batteries for electrical energy storage, Nat. Chem. 7 (2015) 19–29.

[4] K. Chen, D. Xue, Materials chemistry toward electrochemical energy Storage, J. Mater. Chem. A 4 (2016) 7522–7537.

[5] P. Arora, Z. Zhang, Battery separator, Chem. Rev. 104 (2004) 4419–4462.

[6] S.S. Zhang, A review on the separators of liquid electrolyte Li-ion batteries, J. Power Sources 164 (2007) 351–364.

[7] J. Hassoun, S. Panero, B. Scrosati, Recent advances in liquid and polymer lithium-ion batteries, J. Mater. Chem. 17 (2007) 3668–3677.

[8] P.G. Balakrishnan, R. Ramesh, T. Prem Kumar, Safety mechanisms in lithium-ion batteries, J. Power Sources 155 (2006) 401–414.

[9] Y. Xiang, J. Li, J. Lei, D. Liu, Z. Xie, D. Qu, K. Li, T. Deng, H. Tang, Advanced separators for lithium-ion and lithium–sulfur batteries: a review of recent progress, ChemSusChem 9 (2016) 3023–3039.

[10] K.M. Abraham, M. Alamgir, Polymer electrolytes reinforced by Celgard® membranes, J. Electrochem. Soc. 142 (1995) 683–687.

[11] P. Yang, P. Zhang, C. Shi, L. Chen, J. Dai, J. Zhao, The functional separator coated with core–shell structured silica–poly(methyl methacrylate) sub-microspheres for lithium-ion batteries, J. Membr. Sci. 474 (2015) 148–155.

[12] Y. Xie, H. Zou, H. Xiang, R. Xia, D. Liang, P. Shi, S. Dai, H. Wang, Enhancement on the wettability of lithium battery separator toward nonaqueous electrolytes, J. Membr. Sci. 503 (2016) 25–30.

[13] J.-A. Choi, S.H. Kim, D.-W. Kim, Enhancement of thermal stability and cycling performance in lithium-ion cells through the use of ceramic-coated separators, J. Power Sources 195 (2010) 6192–6196.

[14] D. Fu, B. Luan, S. Argue, M.N. Bureau, I.J. Davidson, Nano SiO$_2$ particle formation and deposition on polypropylene separators for lithium-ion batteries, J. Power Sources 206 (2012) 325–333.

[15] C. Shi, P. Zhang, L. Chen, P. Yang, J. Zhao, Effect of a thin ceramic-coating layer on thermal and electrochemical properties of polyethylene separator for lithium-ion batteries, J. Power Sources 270 (2014) 547–553.

[16] D. Yeon, Y. Lee, M.-H. Ryou, Y.M. Lee, New flame-retardant composite separators based on metal hydroxides for lithium-ion batteries, Electrochim. Acta 157 (2015) 282–289.

[17] J.-H. Yoo, W.-K. Shin, S.M. Koo, D.-W. Kim, Lithium-ion polymer cells assembled with a reactive composite separator containing vinyl-functionalized SiO$_2$ particles, J. Power Sources 295 (2015) 149–155.

[18] X. Liang, Y. Yang, X. Jin, Z. Huang, F. Kang, The high performances of SiO$_2$/Al$_2$O$_3$-coated electrospun polyimide fibrous separator for lithium-ion battery, J. Membr. Sci. 493 (2015) 1–7.

[19] H. Jeon, S.Y. Jin, W.H. Park, H. Lee, H.-T. Kim, M.-H. Ryou, Y.M. Lee, Plasma-assisted water-based Al$_2$O$_3$ ceramic coating for polyethylene-based microporous separators for lithium metal secondary batteries, Electrochim. Acta 212 (2016) 649–656.

[20] S.-R. Park, Y.-C. Jung, W.-K. Shin, K. Ho Ahn, C.H. Lee, D.-W. Kim, Cross-linked fibrous composite separator for high performance lithium-ion batteries with enhanced safety, J. Membr. Sci. 527 (2017) 129–136.

[21] H. Xiang, J. Chen, Z. Li, H. Wang, An inorganic membrane as a separator for lithium-ion battery, J. Power Sources 196 (2011) 8651–8655.

[22] Y.-C. Jung, S.-K. Kim, M.-S. Kim, J.-H. Lee, M.-S. Han, D.-H. Kim, W.-C. Shin, M. Ue, D.-W. Kim, Ceramic separators based on Li$^+$-conducting inorganic electrolyte for high-performance lithium-ion batteries with enhanced safety, J. Power Sources 293 (2015) 675–683.

[23] Y. Zhang, Z. Wang, H. Xiang, P. Shi, H. Wang, A thin inorganic composite separator for lithium-ion batteries, J. Membr. Sci. 509 (2016) 19–26.

[24] S.-K. Kim, Y.-C. Jung, D.-H. Kim, W.-C. Shin, M. Ue, D.-W. Kim, Lithium-ion cells assembled with flexible hybrid membrane containing Li$^+$-conducting lithium aluminum germanium phosphate, J. Electrochem. Soc. 163 (2016) A974–A980.

[25] A.L. Michan, B.S. Parimalam, M. Leskes, R.N. Kerber, T. Yoon, C.P. Grey, B.L. Lucht, Fluoroethylene carbonate and vinylene carbonate reduction: understanding lithium-ion battery electrolyte additives and solid electrolyte interphase formation, Chem. Mater. 28 (2016) 8149–8159.

[26] X. Li, G. Cheruvally, J.K. Kim, J.W. Choi, J.H. Ahn, K.W. Kim, H.J. Ahn, Polymer electrolytes based on an electrospun poly(vinylidene fluoride-co-hexafluoropropylene) membrane for lithium batteries, J. Power Sources 167 (2007) 491.

[27] Y. Ding, P. Zhang, Z. Long, Y. Jiang, F. Xu, W. Di, The ionic conductivity and mechanical property of electrospun P(VdF-HFP)/PMMA membranes for lithium ion batteries, J. Membr. Sci. 329 (2009) 56–59.

[28] Y.K. Sun, K.J. Hong, J. Prakash, K. Amine, Electrochemical performance of nano-sized ZnO-coated LiNi$_{0.5}$Mn$_{1.5}$O$_4$ spinel as 5 V materials at elevated temperatures, Electrochem. Commun. 4 (2002) 344–348.

[29] Y. Lin, J. Jin, M. Song, Preparation and characterization of covalent polymer functionalized graphene oxide, J. Mater. Chem. 21 (2011) 3455–3461.

[30] C. Shi, J. Dai, X. Shen, L. Peng, C. Li, X. Wang, P. Zhang, J. Zhao, A high-temperature stable ceramic-coated separator prepared with polyimide binder/Al$_2$O$_3$ particles for lithium-ion batteries, J. Membr. Sci. 517 (2016) 91–99.

[31] Y. Zhai, K. Xiao, J. Yu, B. Ding, Fabrication of hierarchical structured SiO$_2$/polyetherimide-polyurethane nanofibrous separators with high performance for lithium ion batteries, Electrochim. Acta 154 (2015) 219–226.

[32] M.D. Levi, G. Salitra, B. Markovsky, H. Teller, D. Aurbach, U. Heider, L. Heider, Solid-state electrochemical kinetics of Li-ion intercalation into Li$_{1-x}$CoO$_2$: simultaneous application of electroanalytical techniques SSCV, PITT, and EIS, J. Electrochem. Soc. 146 (1999) 1279–1289.

[33] S.S. Zhang, K. Xu, T.R. Jow, Electrochemical impedance study on the low temperature of Li-ion batteries, Electrochim. Acta 49 (2004) 1057–1061.

[34] T. Liu, A. Garsuch, F. Chesneau, B.L. Lucht, Surface phenomena of high energy Li (Ni$_{1/3}$Co$_{1/3}$Mn$_{1/3}$)O$_2$/graphite cells at high temperature and high cutoff voltages, J. Power Sources 269 (2014) 920–926.

[35] C.M. Yang, H.S. Kim, B.K. Na, K.S. Kum, B.W. Cho, Gel-type polymer electrolytes with different types of ceramic fillers and lithium salts for lithium-ion polymer batteries, J. Power Sources 156 (2006) 574–580.

[36] S.J. Lim, Y.S. Kang, D.-W. Kim, Dye-sensitized solar cells with quasi-solid-state cross-linked polymer electrolytes containing aluminum oxide, Electrochim. Acta 56 (2011) 2031–2035.

[37] G.G. Amatucci, J.M. Tarascon, L.C. Klein, Cobalt dissolution in LiCoO$_2$-based non-aqueous rechargeable batteries, Solid State Ion. 83 (1996) 167–173.

[38] S.U. Woo, B.C. Park, C.S. Yoon, S.T. Myung, J. Prakash, Y.K. Sun, Improvement of electrochemical performances of Li [Ni$_{0.8}$Co$_{0.1}$Mn$_{0.1}$] O$_2$ cathode materials by fluorine substitution, J. Electrochem. Soc. 154 (2007) A649–A655.

[39] H. Yang, G.V. Zhuang, P.N. Ross Jr., Thermal stability of LiPF$_6$ salt and Li-ion battery electrolytes containing LiPF$_6$, J. Power Sources 161 (2006) 573–579.

[40] E. Zinigrad, L. Larush-Asraf, J.S. Gnanaraj, M. Sprecher, D. Aurbach, On the thermal stability of LiPF$_6$, Thermochim. Acta 438 (2005) 184–191.

[41] W. Cho, S.M. Kim, J.H. Song, T. Yim, S.G. Woo, K.W. Lee, J.S. Kim, Y.J. Kim, Improved electrochemical and thermal properties of nickel rich LiNi$_{0.6}$Co$_{0.2}$Mn$_{0.2}$O$_2$ cathode materials by SiO$_2$ coating, J. Power Sources 282 (2015) 45–50.

[42] A.M. Stephan, K.S. Nahm, Review on composite polymer electrolytes for lithium batteries, Polymer 47 (2006) 5952–5964.

[43] W. Li, C. Campion, B.L. Lucht, B. Ravdel, J. DiCarlo, K.M. Abraham, Additives for stabilizing LiPF$_6$-based electrolytes against thermal decomposition, J. Electrochem. Soc. 152 (2005) A1361–A1365.